A&A 428, L21–L24 (2004)
DOI: 10.1051/0004-6361:200400096

Astronomy & Astrophysics

Atomic carbon in PSS 2322+1944, a quasar at redshift 4.12⋆

J. Pety[1,2], A. Beelen[3], P. Cox[3], D. Downes[1], A. Omont[4], F. Bertoldi[5], and C. L. Carilli[6]

[1] IRAM, 300 rue de la Piscine, 38406 St-Martin-d'Hères, France
e-mail: pety@iram.fr
[2] LERMA, Observatoire de Paris, 75014 Paris, France
[3] Institut d'Astrophysique Spatiale, Université de Paris Sud, 91405 Orsay Cedex, France
[4] Institut d'Astrophysique de Paris, CNRS and Université de Paris VI, 98bis Bd. Arago, 75014 Paris, France
[5] Max-Planck-Institut für Radioastronomie, Auf dem Hügel 69, 53121 Bonn, Germany
[6] National Radio Astronomy Observatory, PO Box, Socorro, NM 87801, USA

Received 22 September 2004 / Accepted 30 October 2004

Abstract. We report the detection of the $^3P_1 \rightarrow {}^3P_0$ fine-structure line of neutral carbon in the $z = 4.12$ quasar PSS 2322+1944, obtained at the IRAM Plateau de Bure interferometer. The [CI] $^3P_1 - {}^3P_0$ line is detected with a signal-to-noise ratio of ∼6 with a peak intensity of ≈2.5 mJy and a velocity-integrated line flux of 0.81 ± 0.12 Jy km s^{-1}. Assuming an excitation temperature of 43 K (equal to the dust temperature), we derive a mass of neutral carbon (corrected for magnification) of $M_{\rm CI} \approx 1.2 \times 10^7\ M_\odot$. In PSS 2322+1944, the cooling due to C is about 6 times smaller than for CO, whereas the CO and C cooling represents $\approx 10^{-4}$ of the far-infrared continuum and more than half of the cooling due to C^+.

Key words. galaxies: formation – galaxies: starburst – galaxies: high-redshift – quasars: emission lines – quasars: individual: PSS 2322+1944 – cosmology: observations

1. Introduction

With the detection of dust and molecular gas in sources at high redshift, it has become possible to probe the physical conditions of the interstellar medium in galaxies and in the hosts of quasi-stellar objects (QSOs) at cosmological distances. The high-z sources detected in ^{12}CO (to date 30 sources between $1.44 < z < 6.42$ – see, e.g., Greve et al. 2004) have massive reservoirs of warm and dense molecular gas (a few 10^{10}–$10^{11}\ M_\odot$), which are predominantly excited by extreme starbursts with implied star formation rates $\approx 10^3\ M_\odot$ yr^{-1}. Multiline CO studies are available in only a few cases, and the detection of species other than carbon monoxide is reported in only a couple of sources. A remarkable example is the Cloverleaf, a strong gravitationally lensed QSO at $z = 2.56$ where four CO transitions were detected, together with the two fine-structure lines of neutral carbon [CI] (Barvainis et al. 1997; Weiß et al. 2003) and the $J = 1 \rightarrow 0$ transition of HCN (Solomon et al. 2003).

Atomic carbon is an important probe of the neutral dense gas. It is a good tracer of molecular gas in external galaxies and plays a central role in the cooling of the gas (Gérin & Phillips 1998, 2000). In high-z sources, the detection of the [CI] lines enables to obtain further constraints on the physical conditions of the interstellar gas in addition to those obtained from the CO transitions (Weiß et al. 2003), providing useful information on the gas column density, the thermal balance, and the UV illumination.

PSS 2322+1944 is an optically luminous, gravitationally lensed QSO at $z = 4.12$ which was studied in detail both in the dust and radio continuum emission (Omont et al. 2001; Beelen et al. 2004) and in the $J = 5 \rightarrow 4$, $4 \rightarrow 3$, $2 \rightarrow 1$, and $1 \rightarrow 0$ transitions lines of CO (Cox et al. 2002; Carilli et al. 2002). With an apparent far-infrared (FIR) luminosity of $3 \times 10^{13}\ L_\odot$, it harbors a massive reservoir of molecular gas which is the site of active star formation with an implied star formation rate of ∼900 $M_\odot$ yr^{-1}. The CO line emission is resolved into an Einstein Ring with a diameter of 1.″5, a direct indication of lensing. The amplification factor is estimated to be about 3.5. The data are consistent with a disk surrounding the QSO with a radius of 2 kpc and a dynamical mass of a few $10^{10}\ M_\odot$ (Carilli et al. 2003).

The observations of the molecular gas in PSS 2322+1944 provide one of the best examples to date of active star formation in the host galaxy of a luminous, high redshift QSO. The strong CO emission in PSS 2322+1944 makes it a prime target to search for the $^3P_1 \rightarrow {}^3P_0$ transition of [CI] ($\nu_{\rm rest}$ = 492.161 GHz) which, at $z = 4.12$, is shifted into the 3 mm atmospheric window.

Here we report the $^3P_1 \rightarrow {}^3P_0$ [CI] line in PSS 2322+1944. After the detection of [CI] in the Cloverleaf, and, recently, in IRAS FSC 10214 ($z = 2.3$) and SMM J14011+0252 ($z = 2.5$)

⋆ Based on observations obtained with the IRAM Plateau de Bure interferometer.

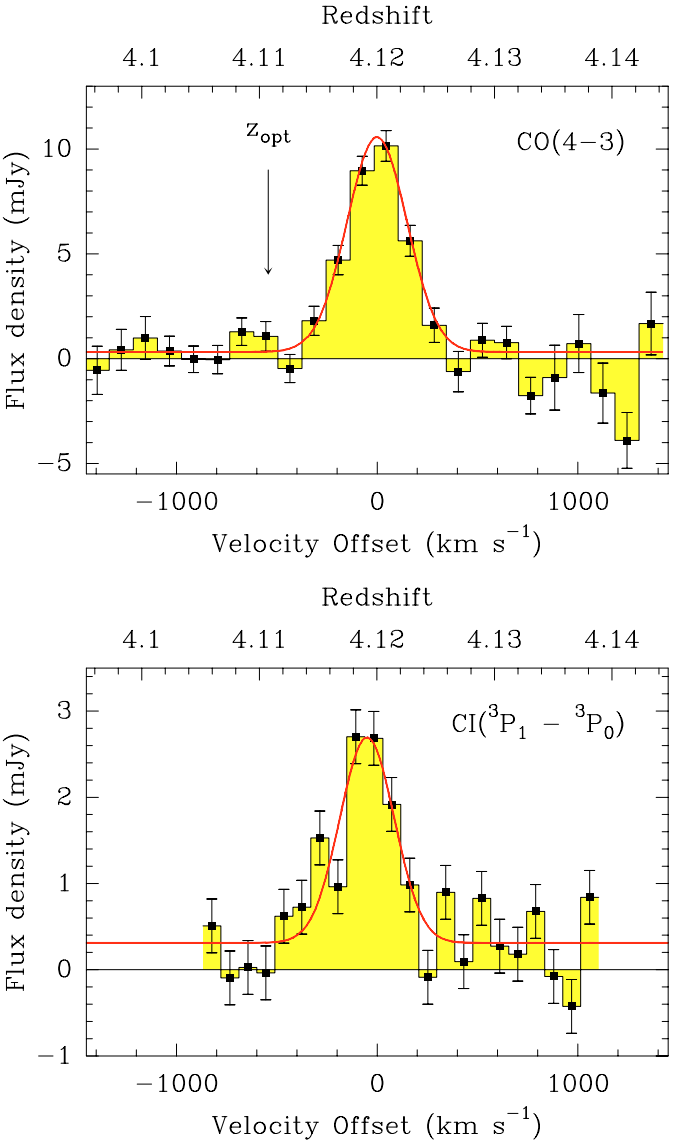

Fig. 1. Observed spectra of the [CI]^{3}P$_1$ → ^{3}P$_0$ (this paper) and CO(J = 4 → 3) lines (from Cox et al. 2002) toward the z = 4.12 quasar PSS 2322+1944. The black horizontal lines show the zero flux density level. The red lines show the results of Gaussian + continuum fits.

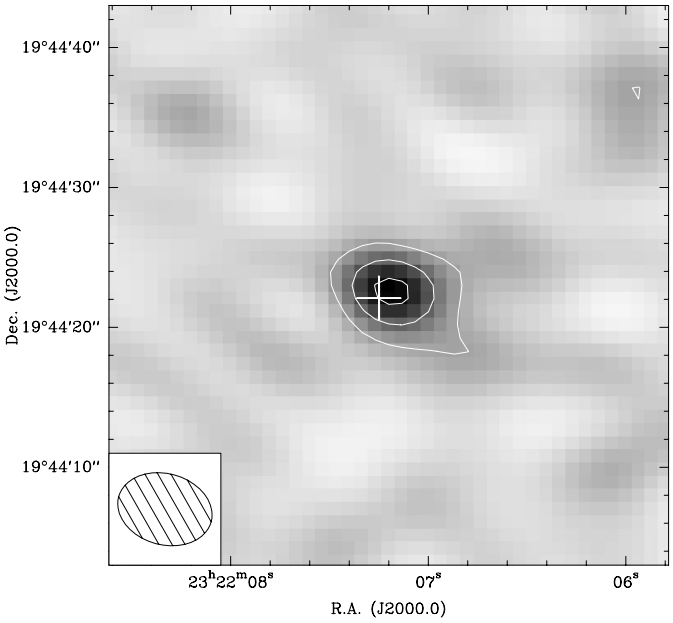

Fig. 2. Map of the [CI] ^{3}P$_1$ → ^{3}P$_0$ velocity-integrated emission toward PSS 2322+1944. The emission is integrated between −400 and +400 km s^{-1}. The white cross indicates the optical position at RA = 23:22:07.25, Dec = 19:44:22.08 (J2000.0). The contours correspond to multiples of 3σ = 0.34 mJy/beam. Negative levels are shown as dotted contours with the same step. The synthesized beam of 6.″8 × 5.″1 (73°) is shown in the lower left corner.

reported by Weiß et al. (2004), these observations represent the fourth clear detection of [CI] in a high-z source. In this paper, we assume the concordance Λ-cosmology with H_0 = 71 km s^{-1} Mpc^{-1}, Ω_Λ = 0.73 and Ω_m = 0.27 (Spergel et al. 2003).

2. Observations and data reduction

Observations of the ^{3}P$_1$ → ^{3}P$_0$ transition of [CI] in PSS 2322+1944 were carried out with the IRAM Plateau de Bure interferometer (PdBI) in a series of observing sessions between July 2002 and June 2004. The total integration time of the useful data is equivalent to 34 h with 6 antennas. In practice, all the observing time was allocated during the summer, when antenna maintenance takes place. The total on-sky integration time amounts to 116 h often with 4 or 5 (and sometimes with 6) antennas.

We used the interferometer in the D configuration. The combined 3.2 mm data result in a synthesized beam of 6.″85 × 5.″09 at a position angle of 73°. The 3 mm receivers were tuned first at the red-shifted frequency of the [CI] ^{3}P$_1$ → ^{3}P$_0$ line, i.e. 96.127 GHz at z = 4.119 and then at 96.063 GHz for the second half of the data. This is the reason why the spectrum is noisier at the very ends of the band (Fig. 1). At those frequencies, the typical SSB system temperatures were ≈150–250 K. The water vapor ranged between 4 and 10 mm on different sessions. The 580 MHz instantaneous IF–bandwidth were observed with a resolution of 1.5 MHz.

All data reduction were done using the GILDAS softwares. Standard calibration methods using close calibrators were applied. The bandpass calibration was done on the quasar 3C 454.3. The amplitude and phase calibration were performed on 3C 454.3 and the nearby quasar 2230+114. Only data with phase noise better than 40 deg were used. The maximum position errors at 3.2 mm introduced by such phase noise is <0.″5. The flux calibration is based on the PdBI primary calibrator MWC 349. The fluxes of 3C 454.3 (resp. 2230+114) varied from 7 to 4 Jy (resp. 4 to 2.4 Jy) during the 3 years observing period.

A standard calibrated *uv* table was produced and analyzed both by direct fits in the *uv* plane (as this avoids the deconvolution step) and by making the deconvolved image shown in Fig. 2. Both methods confirm that the [CI] ^{3}P$_1$ → ^{3}P$_0$ emission is i) detected; ii) not resolved by our observations; and iii) centered on the optical position which is also the phase center

Table 1. Properties of the [CI] and CO(4 → 3) lines observed toward PSS 2322+1944.

Line	$\nu_{\rm rest}$ [GHz]	$\nu_{\rm obs}$ [GHz]	Peak Int. [mJy]	Position [km s^{-1}]	$\Delta v_{\rm FWHM}$ [km s^{-1}]	I [Jy km s^{-1}]	L' [10^{10} K km s^{-1} pc^2]	L [10^8 $L_\odot$]
[CI] $^3P_1 \rightarrow {}^3P_0$	492.161	96.127	2.4	-52 ± 25	319 ± 66	0.81 ± 0.12	3.4 ± 0.5	1.1 ± 0.2
CO $(4 \rightarrow 3)^\dagger$	461.041	90.048	10.3	-3 ± 10	348 ± 40	3.83 ± 0.40	16.3 ± 1.5	5.1 ± 0.5

NOTE. – The CO(4 → 3) data are from Cox et al. (2002). The continuum and the line were fitted separately using an a priori line window (between −400 to +400 km s^{-1}) defined from the high signal-to-noise CO $J = 4 \rightarrow 3$ spectrum. The luminosities are not corrected for the lens amplification ($m = 3.5$).

of the observations. The two latter points allow us to derive the source spectrum from the real part of the average of all the complex visibilities. The main advantage of this method is to directly obtain the spectrum from simple operations instead of applying the usual fitting procedures in the *uv* plane. Any further processing (smoothing, fitting) was performed using the CLASS software.

The final [CI] spectrum at a velocity resolution of 90 km s^{-1} is displayed in Fig. 1 together with the spectrum of the $J = 4 \rightarrow 3$ transition of CO. The image of the [CI] emission is shown in Fig. 2. The [CI] $^3P_1 \rightarrow {}^3P_0$ fine-structure line is clearly detected at the same redshift as the CO emission with a peak flux density of $S_\nu = 2.69 \pm 0.31$ mJy (including the continuum flux of 0.31 mJy). Table 1 summarizes the line parameters derived from continuum + Gaussian fits.

3. Results and discussion

The integrated flux of the [CI] $^3P_1 \rightarrow {}^3P_0$ line is 0.81 ± 0.12 Jy km s^{-1}, a factor of 5 lower than the CO(4 → 3) line. A Gaussian fit yields a line width of 319 ± 66 km s^{-1} and a line center displaced by -50 km s^{-1} relative to CO(4 → 3). Due to the weak signal to noise ratio of the [CI] data, the difference in the line position with the higher quality CO(4 → 3) data should not be over-interpreted. The [CI] line flux implies a line luminosity of $L'_{\rm CI} = 3.4 \pm 0.5 \times 10^{10}$ K km s^{-1} pc^2 or $1.1 \pm 0.2 \times 10^8$ $L_\odot$ (see, e.g., Solomon et al. 1997, for the definition of the line luminosity). The [CI] luminosity in PSS 2322+1944 is thus about a factor 2 lower than in the case of the Cloverleaf where $L'_{\rm CI} = 6.1 \times 10^{10}$ K km s^{-1} pc^2, as derived from the [CI] velocity-integrated flux of Barvainis et al. (1997).

The continuum emission is detected at 96 GHz with 0.31 ± 0.08 mJy, which is consistent for dust emission with the available photometric data at higher frequency. The FIR spectral energy distribution of PSS 2322+1944 is well reproduced with a grey body of temperature 43 ± 6 K and a dust emissivity $\propto \nu^{1.6\pm0.3}$ (Beelen et al. 2004).

The detection of the [CI] $^3P_1 \rightarrow {}^3P_0$ emission line in PSS 2322+1944 allows us to estimate the mass of neutral carbon $M_{\rm CI}$. Since the $^3P_2 \rightarrow {}^3P_1$ transition (at $\nu_{\rm rest}$ = 809.342 GHz) is not observed, we assume that the $^3P_1 \rightarrow {}^3P_0$ transition is optically thin as is the case for the Cloverleaf (Weiß et al. 2003). Under these assumptions, we can express the mass of neutral carbon as a function of $L'_{\rm CI}$

$$M_{\rm CI} = 5.65 \times 10^{-4} \, \frac{Q}{3} \, {\rm e}^{(23.6/T_{\rm ex})} \, L'_{\rm CI(^3P_1 \rightarrow {}^3P_0)} \, M_\odot, \quad (1)$$

where $T_{\rm ex}$ is the excitation temperature and Q is the CI partition function. Assuming that $T_{\rm ex}$ is equal to the temperature of the warm dust $T_{\rm dust} = 43$ K, the mass of neutral carbon in PSS 2322+1944 amounts to $M_{\rm CI} = 4.3 \times 10^7$ $M_\odot$, or 1.2×10^7 $M_\odot$ after correction for lens amplification ($m = 3.5$). Although the excitation temperature of the neutral carbon can be different than $T_{\rm dust}$ (as observed for the Cloverleaf – see Weiß et al. 2003), the derived mass depends only weakly on $T_{\rm ex}$. For a range of [CI] excitation temperatures from 30 to 100 K, the mass of neutral carbon in PSS 2322+1944 would vary from 1.2 to 1.4×10^7 $M_\odot$.

Compared to the mass of molecular gas of $M_{\rm H_2} = 7 \times 10^{10}$ $M_\odot$ after correcting for amplification (Cox et al. 2002; Carilli et al. 2003), the derived mass of [CI] implies a carbon abundance relative to H_2 of [CI]/[H_2] ≈ 3×10^{-5}, indicating near to solar abundances in this high-redshift system. Similar values are derived by Weiß et al. (2004). This relative carbon abundance is close to the maximum value of 2.2×10^{-5} found for Galactic dense molecular clouds with opacities of 4–11 mag, a value which does not vary within a factor of a few for larger $A_{\rm V}$'s (Frerking et al. 1989).

The [CI] $^3P_1 \rightarrow {}^3P_0$ and $^3P_2 \rightarrow {}^3P_1$ lines are major gas coolants. In the Cloverleaf, the $^3P_2 \rightarrow {}^3P_1$ line is 2.2 times stronger than the $^3P_1 \rightarrow {}^3P_0$ line (Weiß et al. 2003). To estimate the carbon cooling, we may assume a similar ratio for PSS 2322+1944. To compare this to the CO cooling, we added the observed CO line luminosities of PSS 2322+1944 up to $J = 9-8$, where for the unobserved transitions we adopt the prediction of the LVG model of Carilli et al. (2002). In PSS 2322+1944, we find that the CO/[CI] luminosity ratio is 6, as compared to a ratio of 20 for the Cloverleaf (see Table 2). However, the total mass of [CI] remains somewhat smaller than that of CO (see Carilli et al. 2002).

Compared to the far-IR luminosity of PSS 2322+1944, $L_{\rm FIR} \sim 8.6 \times 10^{12}$ $L_\odot$ (corrected for lensing), the CO and [CI] cooling represents $\sim 10^{-4}$ of the far-IR continuum, again not very different from the ratio of 4×10^{-4} derived for the Cloverleaf (Table 2). The recent search of the red-shifted [CII] fine-structure line in PSS 2322+1944 implies an upper limit to the [CII] line luminosity of 1.7×10^9 $L_\odot$, a weakness which is typical for high-z IR luminous galaxies (Benford et al. 2004). The CO and C cooling is therefore more than half of the cooling due to C^+. The [CII] line remains the main cooling line of the gas.

Table 2. Comparison of the interstellar gas and dust luminosities in Infrared Luminous Galaxies and in the Galactic Center.

Source	z	$C^{\dagger}$ $[L_\odot]$	$CO^{\dagger\dagger}$ $[L_\odot]$	C^+ $[L_\odot]$	L_{FIR} $[L_\odot]$	CO/C	(C+CO)/L_{FIR}	C^+/L_{FIR}	Ref.
PSS 2322+1944[(a)]	4.12	1.0×10^{8}	6.8×10^{8}	$\leq1.7\times10^{9}$	8.6×10^{12}	6.6	9×10^{-5}	$\leq2\times10^{-4}$	[1]
Cloverleaf[(a)]	2.56	7.1×10^{7}	1.5×10^{9}	–	4.2×10^{12}	21.7	3.9×10^{-4}	–	[2]
Arp220	0.018	1.8×10^{7}	3.9×10^{7}	1.6×10^{9}	1.2×10^{12}	2.2	4.7×10^{-5}	1.3×10^{-3}	[3]
NGC 253	0.0008	1.6×10^{5}	1.6×10^{6}	7.8×10^{6}	1.0×10^{10}	10.0	1.8×10^{-4}	7.8×10^{-4}	[4]
Galactic center[(b)]	–	6.7×10^{4}	2.6×10^{5}	2.6×10^{6}	3.9×10^{8}	3.8	8.4×10^{-4}	6.7×10^{-3}	[5]

NOTE. – † Total C I luminosity; †† CO luminosity up to $J = 8$; [(a)] the luminosities are corrected for lensing: $m = 3.5$ for PSS 2322+1944 (Carilli et al. 2003) and $m = 11$ for the Cloverleaf (Venturini & Solomon 2003); [(b)] the central $5 \times 1\,\mathrm{deg}^2$ of the Galaxy. References: [1] This paper – [2] Weiß et al. (2003), Barvainis et al. (1997), A. Weiß (private communication) – [3] Gérin & Phillips (1998) – [4] Bayet et al. (2004) – [5] Fixsen et al. (1999).

Finally, the [CI] luminosity relative to the integrated far-IR luminosity is a good measure of the intensity of the non-ionizing UV radiation field in galaxies, because in photodissociation regions the column density of neutral carbon is mostly insensitive to the UV field, whereas the far-IR emission is directly proportional to the strength of the UV field (see, e.g., Kaufman et al. 1999; Gérin & Phillips 2000). For PSS 2322+1944, this ratio is $\sim3\times10^{-6}$ indicating a UV radiation field of a few 1000 times larger than in the solar vicinity. Both this ratio and the implied strength of the UV illumination are comparable to the values derived for the other IR luminous galaxies and the galactic center listed in Table 2.

As in the case for local starburst galaxies such as NGC 253, CO is a more important coolant than C in both PSS 2322+1944 and the Cloverleaf by about one order of magnitude (Table 2) – see also Schilke et al. (1993) and Bayet et al. (2004). Similarly, in starburst galaxies or in galactic nuclei (including the Milky Way), the molecular gas is warm therefore populating the higher CO levels which contribute to the cooling.

The detection of the red-shifted [CI] $^3P_1 \rightarrow {}^3P_0$ transition line in the gravitationally lensed $z = 4.12$ QSO PSS 2322+1944 enables to further constrain the physical conditions of the neutral gas and to compare the major line (C, CO and C^+) and far-IR luminosities in this high-z galaxy. Together with the recent [CI] detections in other sources at high redshift (Weiß et al. 2004), these results illustrate the potential of studying neutral carbon or species other than CO in high-z sources, a field which will clearly fully develop as soon as more sensitive submillimeter arrays, such as the Atacama Large Millimeter Array (ALMA), will become operational.

Acknowledgements. We thank the IRAM Plateau de Bure staff for their support in the observations. IRAM is supported by INSU/CNRS (France), MPG (Germany), and IGN (Spain). Estelle Bayet and the referee, Dr. Phil M. Solomon, are kindly acknowledged for helpful comments.

References

Barvainis, R., Maloney, P., Antonucci, R., & Alloin, D. 1997, ApJ, 484, 695
Bayet, E., Gérin, M., Phillips, T. G., & Contursi, A. 2004, A&A, 427, 45
Beelen, A., Benford, D., Cox, P., et al. 2004, ApJ, submitted
Benford, D., Cox, P., et al. 2004, ApJ, submitted
Bertoldi, F., Carilli, C., Cox, P., et al. 2003a, A&A, 406, L55
Bertoldi, F., Cox, P., Neri, R., et al. 2003b, A&A, 409, L47
Carilli, C. L., Cox, P., Bertoldi, F., et al. 2002, ApJ, 575, 145
Carilli, C. L., Lewis, G. F., Djorgovski, S. G., et al. 2003, Science, 300, 773
Cox, P., Omont, A., Djorgovski, S., et al. 2002, A&A, 387, 406
Gérin, M., & Phillips T. G. 1998, ApJ, 509, L17
Gérin, M., & Phillips T. G. 2000, ApJ, 537, 644
Greve, T., Bertoldi, F., Smail, I., et al. 2004, MNRAS, submitted
Fixsen, D. J., Bennett, C. L., & Mather, J. C. 1999, ApJ, 526, 207
Frerking, M. A., Keene, J., Blake, G. A., & Phillips, T. G. 1989, ApJ, 344, 311
Kaufman, M. J., Wolfire, M. G., Hollenbach, D. J., & Luhman, M. L. 1999, ApJ, 527, 795
Omont, A., Cox, P., Bertoldi, F. 2001, A&A, 374, 371
Schilke, P., Carlstrom, J. E., Keene, J., & Phillips, T. G. 1993, ApJ, 417, L67
Solomon, P. M., Downes, D., Radford, S. J., & Barrett, J. W. 1997, ApJ, 478, 14
Solomon, P. M., Vanden Bout, P. A., Carilli, C. L., & Guélin, M. 2003, Nature, 426, 636
Spergel, D. N., Verde, L., Peiris, H., et al. 2003, ApJS, 148,175
Venturini, S., & Solomon, P. M. 2003, ApJ, 590, 740
Weiß, A., Henkel, C., Downes, D., & Walter, F. 2003, A&A, 409, L41
Weiß, A., Downes, D., Henkel, C., & Walter, F. 2004, A&A, in press